TISSUE ENGINEERING: Part A
Volume 15, Number 11, 2009

DOI: 10.1089/ten.tea.2009.0141

**Original Article**

# Substrate-Induced Assembly of Fibronectin into Networks: Influence of Surface Chemistry and Effect on Osteoblast Adhesion

Patricia Rico, Ph.D.,[1,2,*] José Carlos Rodríguez Hernández, Ph.D.,[1,2,*] David Moratal, Ph.D.,[1] George Altankov, M.D., Ph.D.,[3,4] Manuel Monleón Pradas, Ph.D.,[1,2,5] and Manuel Salmerón-Sánchez, Ph.D.[1,2,5]

The influence of surface chemistry—substrates with controlled surface density of −OH groups—on fibronectin (FN) conformation and distribution is directly observed by atomic force microscopy (AFM). FN fibrillogenesis, which is known to be a process triggered by interaction with integrins, is shown in our case to be induced by the substrate (in absence of cells), which is able to enhance FN–FN interactions leading to the formation of a protein network on the material surface. This phenomenon depends both on surface chemistry and protein concentration. The level of the FN fibrillogenesis was quantified by calculating the fractal dimension of the adsorbed protein from image analysis of the AFM results. The total amount of adsorbed FN is obtained by making use of a methodology that employs Western blotting combined with image analysis of the corresponding protein bands, with the lowest sensitivity threshold equal to 15 ng of adsorbed protein. Further, FN adsorption is correlated to human osteoblast adhesion through morphology and actin cytoskeleton formation. Actin polymerization is in need of the formation of the protein network on the substrate's surface. Cell morphology is more rounded (as quantified by calculating the circularity of the cells by image analysis) when the degree of FN fibrillogenesis on the substrate is lower.

## Introduction

Cell adhesion involves complex physicochemical phenomena in which different biological molecules participate: extracellular matrix (ECM) proteins, cell membrane proteins, and cytoskeleton proteins, all interact to convey information, transcribe factors, and regulate gene expression.[1] Cell adhesion to synthetic materials is mediated by ECM proteins (including fibronectin [FN], laminin, and vitronectin) that adsorb on the substrate upon contact with physiological fluids *in vivo* or culture medium *in vitro*.[2] The concentration, distribution, and mobility of the adsorbed protein layer on a surface play a fundamental role in the biofunctionality of a synthetic material and are clue factors to understand the biological response of a substrate.

Protein adsorption on material surfaces is a process driven both by the intensity of the energetic interactions between the molecular groups of the substrate's surface and of the protein (i.e., hydrogen bonding, electrostatic, van der Waals interactions) and by entropic changes as a consequence of the unfolding of the protein as bound water is released from the surface.[3,4] Clearly, the amount of protein adsorbed and its conformation depend on the chemical groups of the substrate, which determine the energetic and entropic interactions with the adsorbed proteins. Protein adsorption on different substrates has been extensively investigated in the literature by different techniques. FN, albumin, laminin, collagen, lysozyme, fibrinogen, hemoglobin, and several other proteins were adsorbed on different substrates—most of the time, model surfaces such as mica, glass, and self-assembled monolayers—and were investigated by different techniques that include atomic force microscopy, ellipsometry, quartz crystal microbalance, sodium dodecyl sulfate gel electrophoresis, Fourier Transform Infrared (FT-IR) spectroscopic imaging, electron microscopy, and fluorescence probe techniques.[5–14]

FN is a glycoprotein found in blood, extracellular fluids, and connective tissues and attached to the cell surfaces. Both

[1]Center for Biomaterials and Tissue Engineering, Universidad Politécnica de Valencia, Valencia, Spain.
[2]Regenerative Medicine Unit, Centro de Investigación Príncipe Felipe, Valencia, Spain.
[3]Institut de Bioenginyeria de Catalunya, Barcelona, Spain.
[4]Institució Catalana de Recerca i Estudis Avançats (ICREA), Barcelona, Spain.
[5]Networking Research Center on Bioengineering, Biomaterials and Nanomedicine (CIBER-BBN), Valencia, Spain.
*These two authors contributed equally to this work.

plasma FN and the cell surface forms are dimers, consisting of two subunits of 220 kDa, linked by a single disulfide bond near the carboxyl termini.[15,16] The importance of FN as a mediator of cell adhesion to a substrate was recognized earlier.[17] Since then, many studies have shown the role of FN in promoting cell adhesion and regulating cell survival and phenotype expression on different surfaces.[5,18–23] It has been stressed that, for a fixed surface chemistry, the initial density of integrin–FN bonds is proportional to the surface density of adsorbed FN[18]; moreover, the nature of the surface chemistry is able to modulate FN conformation.[5] It has been suggested that FN adsorbs preferentially on hydrophobic surfaces[19] and that it undergoes greater extension of its dimer arms on hydrophilic glass,[20] in a conformation that favors the binding of antibodies[22] and strength the cell–material interaction.[24] Even the micro/nano surface roughness has been shown to influence FN adsorption.[25,26]

This work investigates FN adsorption on model substrates in which the surface density of hydroxyl groups can be modulated as an independent parameter. The total amount of protein adsorbed on each substrate is quantified by a methodology that includes Western blotting combined with image analysis of the characteristic protein bands. The proposed methodology allows one to quantify in a very reproducible way down to 15 ng of the protein. Protein distribution on each surface is directly observed by making use of atomic force microscopy (AFM). We demonstrate substrate-induced FN fibrillogenesis: we show and quantify (by means of image analysis of the AFM pictures) the formation of the protein network on the synthetic substrate induced solely by its surface chemistry, not initiated by any FN–integrin interactions.[27] The influence of protein density and protein distribution on the initial adsorption of human osteoblasts adhesion is investigated after 6 h of culture.

## Materials and Methods

### Materials

Copolymer sheets were obtained by polymerization of a solution of both monomers ethyl acrylate (Aldrich, 99% pure, Barcelona, Spain) and hydroxyethyl acrylate (HEA; Aldrich, 96% pure), with the desired proportion, using 0.1 wt% of benzoin (Scharlau, 98% pure, Barcelona, Spain) as photoinitiator and a 2 wt% of ethyleneglycol dimethacrylate (Aldrich, 98% pure) as crosslinking agent. The polymerization was carried out up to limiting conversion. Five monomer feed compositions were chosen, given by the weight fraction of HEA in the initial mixture of 1, 0.7, 0.5, 0.3, and 0 ($-OH_x$ refers to the sample with fraction $x$ of HEA in the copolymer). After polymerization, low molecular mass substances were extracted from the material by boiling in ethanol for 24 h and then drying *in vacuo* to constant weight. The equilibrium water content (mass of water absorbed referred to the dry mass of the substrate) was measured by weighing the sample after immersion in water for 3 days (Mettler Toledo AX205, Greifensee, Switzerland). The water contact angle (using a Dataphysics OCA, Filderstadt, Germany) was measured for the different substrates by the sessile drop method. The volume of the drop was 100 μL, and the measurement was taken after 5 s of substrate–water contact.

Small disks (approximately 5-mm diameter and 1-mm thickness) were cut from the polymerized sheets to be used in the protein adsorption and cell adhesion studies. The samples were sterilized with gamma radiation (25 kGy) before the experiments.

### Atomic force microscopy

AFM experiments were performed using a Multimode AFM equipped with NanoScope IIIa controller from Veeco (Santa Barbara, CA) operating in tapping mode in air; the Nanoscope 5.30r2 software version was used. Si-cantilevers from Veeco (Manchester, UK) were used with force constant of 2.8 N/m and resonance frequency of 75 kHz. The phase signal was set to zero at a frequency 5–10% lower than the resonance one. Drive amplitude was 200 mV and the amplitude setpoint $A_{sp}$ was 1.4 V. The ratio between the amplitude setpoint and the free amplitude $A_{sp}/A_0$ was kept equal to 0.7.

FN from human plasma (Sigma, Barcelona, Spain) was adsorbed on the different substrates by immersing the material sheets in 20 μg/mL phosphate buffered saline (PBS) solution for 10 min (the adsorption time was selected to better identify the layer of protein directly in contact with the substrate). Then, the sample was rinsed three times in PBS to eliminate nonadsorbed protein and dried by exposing its surface to a nitrogen flow for a few minutes.

The influence of the concentration of the initial protein solution on the conformation of the adsorbed protein was investigated by immersing the ethyl acrylate sheet ($-OH_0$) in protein solutions of different concentrations: 2, 2.5, 3.3, 5, and 20 μg/mL.

### Western blotting

Samples were placed in a 96-well tissue culture plate and were soaked in PBS 1× for 12 h at 37°C before protein coating. FN from human plasma (Sigma) was adsorbed on the different substrates by immersing the materials' disks in (10, 20, and 29 μg/mL) PBS solution for 12 h at 37°C.

To quantify the amount of adsorbed protein, we quantified the remaining protein in the supernatant, that is, the amount of protein that remained in solution without adsorbing on the material surface. Different aliquots of nonadsorbed protein on substrates were subjected to 5%-sodium dodecyl sulfate polyacrylamide gel electrophoresis, using Laemmli buffer 2× and denaturing standard conditions. Proteins were transferred to a positively charged polyvinylidene difluoride nylon membrane (GE Healthcare, Valencia, Spain) using a semidry transfer cell system (Biorad, Madrid, Spain), and blocked by immersion in 5% skimmed milk in PBS for 1 h at room temperature. The blot was incubated with anti-human FN polyclonal antibody (developed in rabbit; Sigma) (1:500) in PBS containing 0.1% Tween 20 and 2% skimmed milk for 1 h at room temperature and washed three times (10 min for each wash) with PBS containing 0.1% Tween 20 and 2% skimmed milk. The blot was subsequently incubated in horseradish peroxidase–conjugated donkey anti-rabbit immunoglobulin G (GE Healthcare) diluted 1:20,000 in PBS containing Tween 20 and 2% milk (1 h at room temperature).

The enhanced chemiluminescence detection system (GE Healthcare) was used according to the manufacturer's instruction before exposing the blot to X-ray film for 1 min.

### Image processing

All image processing and analysis was done using an in-house software developed under MATLAB R2006a (The MathWorks, Inc., Natick, MA).

All the Western blotting bands were digitized using the same scanner (Epson Stylus Photo RX500; Seiko–Epson, Nagano, Japan) and the same scan parameters: 8-bit gray scale image and 300 dots per inch. The digitized images were binarized using the Otsu's method,[28] which chooses the threshold that minimizes the intraclass variance of the thresholded black and white pixels, to create a mask that automatically selected the edge of each Western blot band. This mask was applied to a negative version of the original scanned picture, providing a resulting image that contained only the Western bands. The last step of the process consisted finally in adding all the pixels that conformed each band correctly weighted by their intensity level.

The degree of connectivity of the protein adsorbed on the substrate was studied using fractal techniques. Our Fractal analysis was based on the calculation of the Fractal dimension parameter ($D$) of each image using the box-counting algorithm that consisted of superposing a grid of a square edge $\lambda$ on the image and counting the squares containing boundaries ($N$); this process was repeated with other values of square edge.[29] Different values of the fraction $\ln(N)/\ln(\lambda)$ were obtained determining a straight line whose slope $m$ is related to Fractal dimension $D$ by $D = -m$.[30,31] Before applying the box-counting algorithm, the image was grayscaled and binarized using the Otsu's method. The contour of the protein was automatically detected in this binarized version of the image, and finally the Fractal dimension was calculated on this image applying the box-counting algorithm.

The shape of the cells was determined through the circularity parameter. This parameter gives an indication of the roundness of the cytoskeleton, and its value is calculated as $(4\times\pi\times\text{area})/(\text{perimeter}^2)$.[32,33] Circles have the greatest area-to-perimeter ratio, and this formula will approach a value of 1 for a perfect circle. Circularity is less than 1 for any other shape, and it indicates the roundness of the analyzed object.

For determining the circularity of the cytoskeleton, several steps were performed on the original fluorescence images: (i) the images were grayscaled and their histograms were equalized, providing an output grayscale image with its intensity values evenly distributed throughout the intensity range. (ii) The cytoskeleton was then detected (segmented), since the cytoskeleton differed greatly in contrast from the background image, a gradient-magnitude method (Sobel)[32–34] was applied to the image, and once the gradient image was calculated, a binary mask was created containing the segmented cytoskeleton. (iii) Compared to the original image, the binary gradient mask showed gaps in the lines surrounding the cytoskeleton (the outline of the object of interest was not completely delineated). These linear gaps disappeared when the Sobel image was dilated using linear structuring elements (a vertical structuring element followed by an horizontal one). (iv) Finally, once the dilated gradient mask showed the shape of the cytoskeleton very nicely, the area and the perimeter were easily calculated, providing the circularity of cytoskeleton.

### *Cell culture*

Human osteoblast cells were obtained from the ECACC Cell bank (Wiltshire, UK). Before seeding on FN-coated substrates, osteoblasts were maintained in Dulbecco's modified Eagle's medium (Invitrogen, Barcelona, Spain) supplemented with 10% fetal bovine serum and 1% penicillin–streptomycin, and passaged every 9 days using standard techniques.

Sample disks (5-mm diameter) were placed in a 96-well tissue culture plate and were soaked in PBS 1× for 12 h at 37°C before coating with FN 20 μg/mL (12 h at 37°C). Then, 50,000 cells of the osteoblasts culture were placed onto each substrate and were maintained at 37°C in a humidified atmosphere under 5% $CO_2$ for 6 h in a serum-free medium (Dulbecco's modified Eagle's medium containing 1g/L D-Glucose, L-Glutamine, Pyruvate, and 1% penicillin–streptomycin). Besides, early stages of cell adhesion were followed on the most hydrophobic substrate (after 30, 90, and 180 min). Each experiment was performed in triplicate.

### *Immunofluorescence and cytoskeleton observation*

Cells were washed in Dulbecco's PBS (DPBS; Invitrogen) and fixed in formalin solution 10% (Sigma) at 4°C for 1 h. Afterward, the samples were rinsed with DPBS and a permeabilizing buffer (10.3 g sucrose, 0.292 g NaCl, 0.06 g $MgCl_2$, 0.476 g HEPES buffer, and 0.5 mL Triton X, in 100 mL water, pH 7.2) was added at room temperature for 5 min. To reduce the background signal, the samples were then incubated in 2% bovine serum albumin/DPBS (Sigma) at room temperature with BODIPY® FL phallacidin (2–3 units/sample; Molecular Probes, Barcelona, Spain). The samples were then rinsed in DPBS three times for 5 min each. Finally, the samples were washed before being mounted in Vectashield containing 4′,6-diamidino-2-phenylindole staining (Vector Laboratories, Barcelona, Spain). A Leica DM6000B fluorescent microscope (Leica, Barcelona, Spain) was used. The image system was equipped with a Leica DFC350FX camera.

## Results

Table 1 shows the equilibrium water content and the water contact angle for the different substrates. Both magnitudes quantify the hydrophilicity and wettability of the substrates, which are well correlated with the fraction of −OH groups.

### *Protein quantification by Western blotting*

The amount of FN adsorbed on the different surfaces was quantified by image analysis of the Western blot bands. Calibration curves were built with known amounts of FN charged in the gel, that is, different concentrations of the protein solution. Figure 1a shows the characteristic FN bands

Table 1. Equilibrium Water Content and Water Contact Angle for the Different Substrates

| $x_{OH}$ | *Equilibrium water content* | *Water contact angle (°)* |
|---|---|---|
| 0 (pure PEA) | $1.7 \pm 0.4$ | $89 \pm 1$ |
| 0.3 | $7.6 \pm 0.9$ | $80 \pm 2$ |
| 0.5 | $18.2 \pm 1.7$ | $67 \pm 1$ |
| 0.7 | $40.6 \pm 0.4$ | $55 \pm 1$ |
| 1 (pure PHEA) | $134 \pm 5$ | $45 \pm 2$ |

PEA, poly(ethyl acrylate); PHEA, poly(hydroxyethyl acrylate).

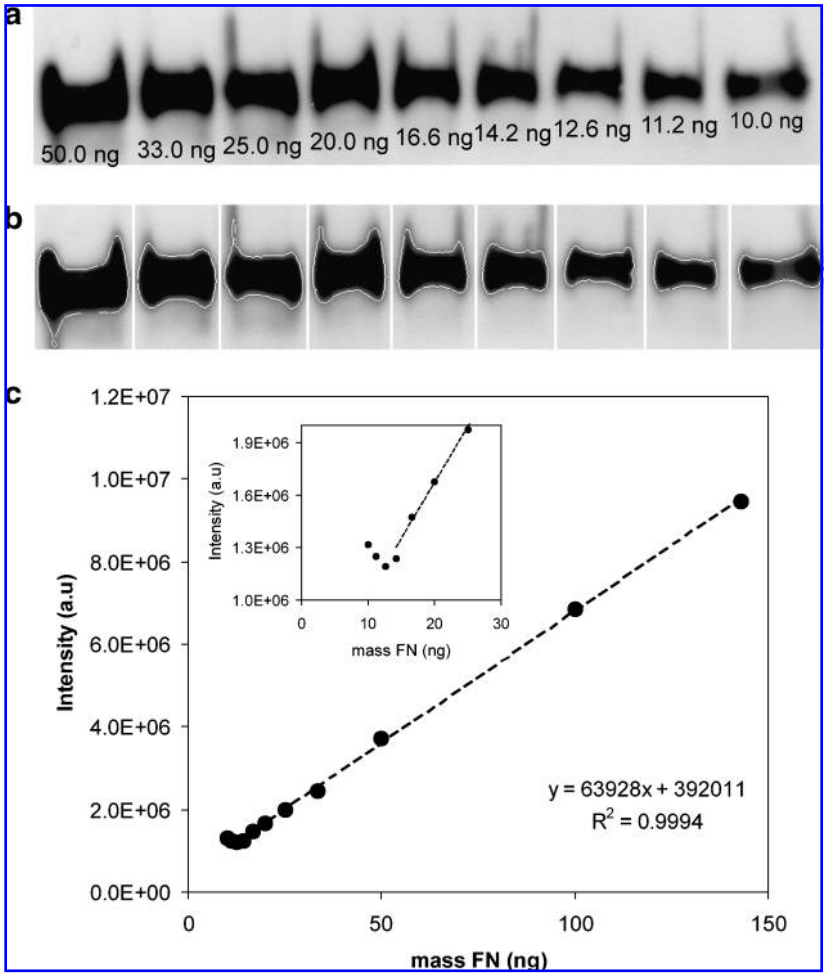


**FIG. 1.** Calibration procedure for Western blot quantification of fibronectin (FN). (**a**) Characteristic Western blot band for different amounts of FN in the experiment as indicated below each band. (**b**) Image analysis of the experimental bands. The edge of each band and its optical intensity were quantified following Otsu's method, which allows one to suppress the observer influence. (**c**) Band intensity versus FN mass calibration curve.

associated to different amounts of the protein in the gel (between 1 and 30 μg/mL that correspond to 10 and 50 ng of FN charged in the gel, respectively). The dimension of the band decreases as the amount of FN decreases. The edge of each band detected by means of the Otsus' algorithm[28] is depicted together with the original bands in Figure 1b. The possibility of identifying the contour of the band in a systematic and objective way (i.e., independent of the observer) is one of the strengths of the algorithm developed to analyze Western blot bands. Figure 1c shows the calibration curve obtained from a set of four calibration experiments like the one shown in Figure 1a. The optical intensity of the bands increases linearly as the amount of protein loaded in the gel increases. There is a lower limit to the sensitivity that is established to be 15 ng from Figure 1c: lower amounts of protein in the gel do not correlate in a monotonous way with the optical density measured (see the inset in Fig. 1c).

The calibration curve in Figure 1c has been employed to quantify the amount of protein adsorbed on the different substrates. Each experiment included two calibration points so that the position of the whole calibration curve could be checked each time. Figure 2 shows the results of the experiment on the different substrates as a function of the −OH fraction within the material. Three different curves have been included corresponding to FN adsorption from three concentrations in the original solution: 10, 20, and 29 μg/mL. As expected, for a fixed −OH fraction, the higher the concentration of the protein solution, the higher the adsorbed protein on the substrate. There is no saturation of the surface for the selected solution concentrations. For a fixed protein concentration of the protein solution, the adsorbed protein depends nonmonotonically on the −OH density of the substrate, and FN surface density shows a minimum at approximately $x_{OH} = 0.5$. Both higher and lower concentrations of hydroxyl groups in the substrate result in higher amounts of the adsorbed protein. For all concentrations of the original solution, the highest protein adsorption occurs on the most hydrophilic substrate.

### *Protein conformation by AFM*

Figure 3 shows the AFM images of the FN adsorbed on the poly(ethyl acrylate) (PEA) substrate after 10 min from protein solutions of different concentrations (as indicated in the figure caption). The FN conformation on the surface depends on the concentration of the initial protein solution from which the protein is adsorbed. The lowest concentration (2 μg/mL, Fig. 3a) results in isolated globular FN molecules homogeneously distributed on the material. For a concentration of 2.5 μg/mL (Fig. 3b) globular protein molecules are still observed, but with a higher density. Interestingly, there are some areas on the material surface where several FN globular molecules tend to align, suggesting the initial formation of intermolecular connections (Fig. 3f shows the

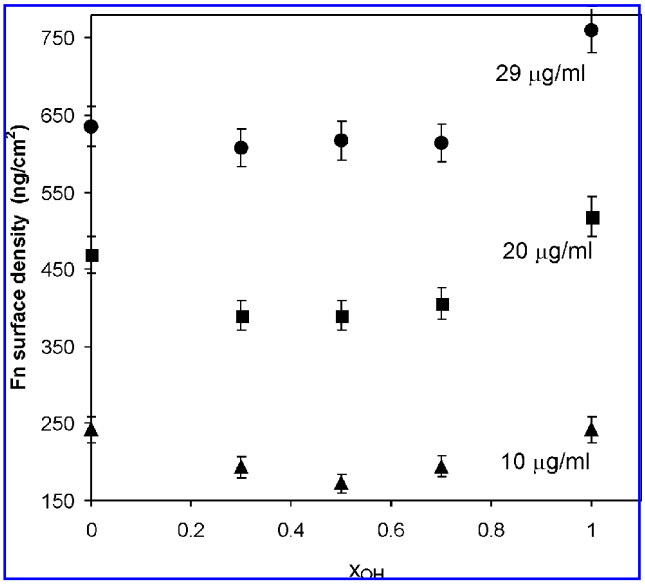


**FIG. 2.** FN surface density as a function of the fraction of −OH groups in the substrate, as measured by the mass fraction of hydroxyethyl acrylate monomer in the copolymer ($x_{OH}$). FN was adsorbed for 12 h from three different solutions of concentrations (▲) 10 μg/mL, (■) 20 μg/mL, and (●) 29 μg/mL.

magnification of the area marked by the arrow in Fig. 3b). FN conformation in Figure 3c suggests the formation of a protein network on the material when FN was adsorbed from a solution of concentration 3.3 μg/mL. When this concentration increases to 5 μg/mL the network is well established (Fig. 3d). Protein adsorption from higher solution concentrations gives rise to the formation of FN networks on the material with higher crosslink density, that is, higher number of crosslinked points and lower distance between them, as for the 20 μg/mL solution concentration (Fig. 3e). The interconnectivity of the protein molecules adsorbed on the substrate's surface was quantified by means of the calculation of the fractal dimension from AFM images (Fig. 3).[29–31] Table 2 includes the fractal dimension that increases as the protein network is formed on the substrate.

Surface density of −OH groups influences FN conformation on the substrates. Figure 4 shows protein conformation and distribution after adsorption on the different substrates from a 20-μg/mL protein solution, which is the concentration typically employed when coating a substrate with the protein for cell culture purposes.[5,18,23] The more hydrophobic surfaces induce the formation of protein networks, whose density decreases as the fraction of −OH groups increases.

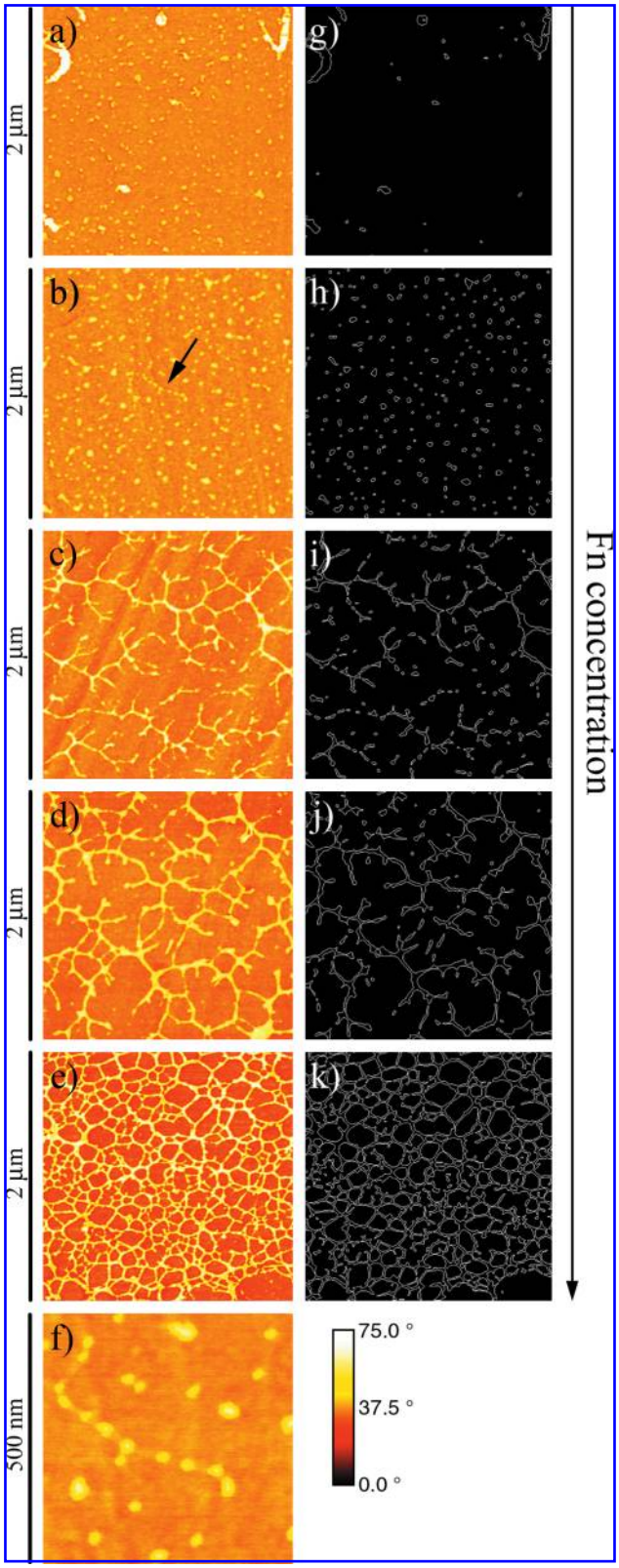


**FIG. 3.** FN conformation on PEA as observed by the phase magnitude in atomic force microscopy (AFM). The protein was adsorbed for 10 min from different solutions of concentrations (**a**) 2 μg/mL, (**b**) 2.5 μg/mL, (**c**) 3.3 μg/mL, (**d**) 5 μg/mL, and (**e**) 20 μg/mL, and (**f**) shows at a higher magnification the sequence marked by the arrow in (**b**). Image analysis of the AFM pictures allows one to obtain the corresponding sketelonised pictures shown in (**g–k**) from which the fractal dimension is calculated to quantify the degree of FN interconnection. Color images available online at www.liebertonline.com/ten.

Table 2. Interconnectivity of the Protein Network on the Most Hydrophobic Substrate's Surface (poly(ethyl acrylate) [PEA], $x_{OH} = 0$) as a Function of Protein Concentration of the Solution Quantified by the Fractal Dimension Calculated from Atomic Force Microscopy Contour Images Depicted in Figure 3

| *Concentration (μg/mL)* | *Fractal dimension* |
|---|---|
| 2.0 | 1.15 |
| 2.5 | 1.35 |
| 3.3 | 1.44 |
| 5.0 | 1.49 |
| 20 | 1.62 |

FN network is well developed on the PEA ($-OH_0$) and the $-OH_{10}$ substrates (Fig. 4a, b). On the $-OH_{20}$ substrate the network is still present, but some crosslinking points are lost, as shown in Figure 4c, and the crosslinking density is lower compared to the adsorbed protein on PEA and $-OH_{10}$ (Fig. 4c). Protein aggregates with elongated shape are still formed on the $-OH_{30}$ surface, but only weakly connected protein filaments are identified (Fig. 4d). A higher amount of hydroxyl groups (from $x_{OH} = 0.5$ on) prevents the formation of a protein network on the materials surface, and only disperse (micro) aggregates of the protein are observed on the $-OH_{50}$, $-OH_{70}$, and poly(hydroxyethyl acrylate) (PHEA) substrates. The surface density of these globular FN aggregates seems to increase with the fraction of hydroxyl groups from $x_{OH} = 0.5$ to 1 (see, e.g., Fig. 4e–g). The extent of the protein network on the different substrates was quantified by calculation of the fractal dimension (Table 3).

### *Osteoblast adhesion*

Substrates were coated for 12 h with FN solutions (20 μg/mL); then, the development of F-actin fibers was investigated as a function of the $-OH$ surface density after 6 h

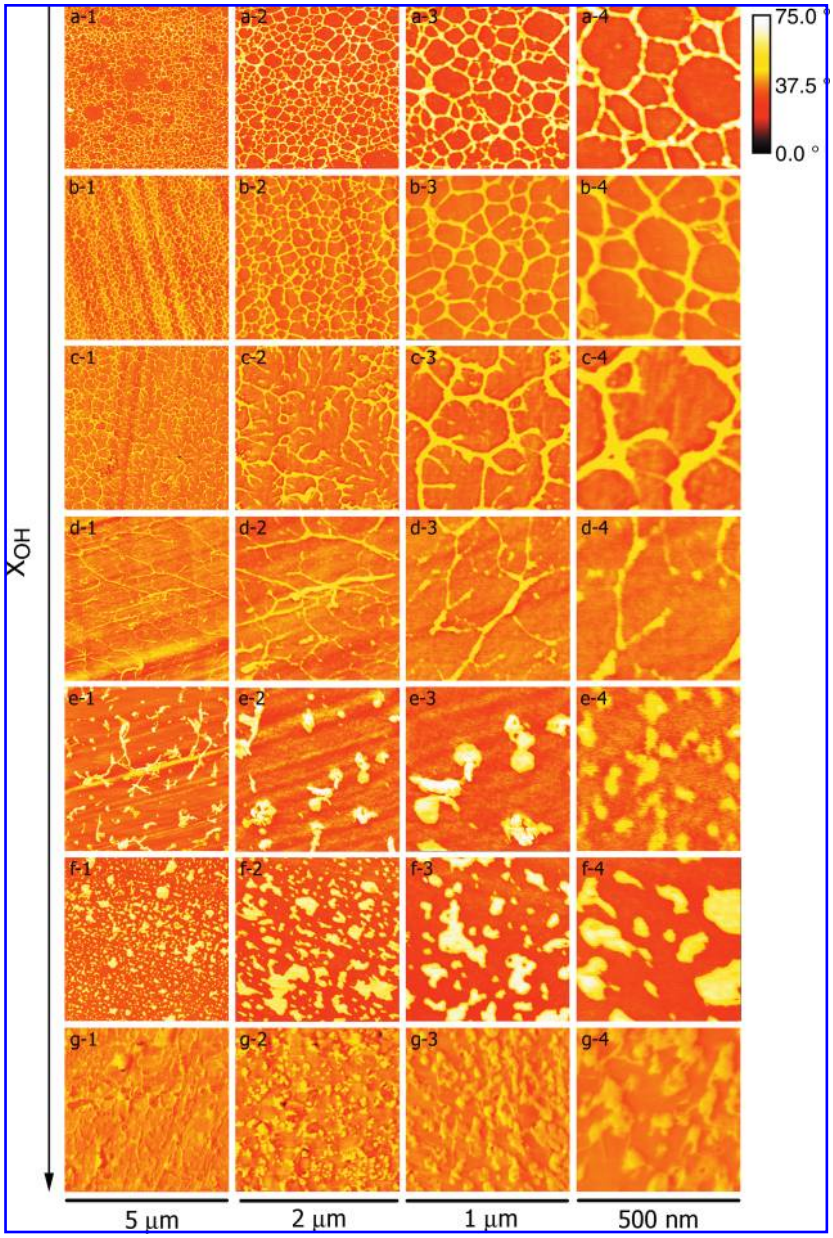


**FIG. 4.** FN conformation as revealed by the phase magnitude in AFM. The protein was adsorbed for 10 min from a solution of concentration 20 μg/mL on substrates with increasing fraction of $-OH$ groups. (**a**) poly(ethyl acrylate) (PEA), $x_{OH} = 0$, (**b**) $x_{OH} = 0.10$, (**c**) $x_{OH} = 0.20$, (**d**) $x_{OH} = 0.30$, (**e**) $x_{OH} = 0.50$, (**f**) $x_{OH} = 0.70$, and (**g**) poly(hydroxyethyl acrylate) (PHEA), $x_{OH} = 1$ ($x_{OH}$ is the mass fraction of hydroxyethyl acrylate monomer in the copolymer). Color images available online at www.liebertonline.com/ten.

Table 3. Interconnectivity of the Protein Network on the Different Substrate's Surface (as a Function of OH Surface Density) Quantified by the Fractal Dimension Calculated on Contour Images Extracted from Atomic Force Microscopy Images Depicted in Figure 4

| $x_{OH}$ | *Fractal dimension/2 μm* |
|---|---|
| 0.0 | 1.62 |
| 0.1 | 1.59 |
| 0.2 | 1.52 |
| 0.3 | 1.44 |

Calculation was performed on the $2\times2\,\mu m^2$ images. Only those substrates on which fibronectin fibrillogenesis takes place are included.

of cell culture on the protein-coated surfaces. Drying the surface of the sample (as it is done for AFM experiments) before cell culture was shown not to influence results. The state of the actin cytoskeleton depended strongly on the amount of −OH groups in the samples through the conformation of the previously adsorbed FN. F-actin cytoskeleton was well developed in cells cultured on the hydrophobic substrate (Fig. 5a). No actin fibers were found in cells cultured on the other samples, but the degree of formation of the actin cytoskeleton was not the same. Initial trends of fiber formation are hardly visible in cells cultured on the $-OH_{30}$ sample, as marked by the arrows in Figure 5b. Substrates with higher amounts of hydroxyl groups ($-OH_{50}$, $-OH_{70}$, and $-OH_{100}$) show green shadows without any trace of F-actin cables. The ring around the cell periphery, characteristic of the initial stages of F-actin polymerization,[35] is clearly visible in the sample with the highest fraction of −OH groups (Fig. 5e). Moreover, cell morphology depends strongly on the −OH groups in the samples: cells tend to be more rounded as the hydrophilicity of the substrate increases. The morphologic parameter circularity was calculated on some selected cells adhered to each substrate by image analysis (Fig. 5), and it is displayed in Table 4.[32–34]

Early stages of cell adhesion on the most hydrophobic substrate was further investigated by following the formation of the actin cytoskeleton after 30, 90, and 180 min. Figure 6a shows round cell morphology lacking any acting organization and many philopodia well distributed along the cell periphery. After 90 min, the F-actin cytoskeleton is visible and cell spreading has started, even if cell area does not change appreciably. After 180 min, F-actin cables are completely visible and cell spreading on the substrate has been completed.

## Discussion

Cell adhesion on a substrate is mediated by ECM proteins, mainly FN, adsorbed onto its surface. The cell–protein–material interaction is modulated by the distribution, conformation, and strength of adhesion between the ECM protein and the substrate.[35,36] FN conformation on a synthetic material has been shown to depend on the surface chemistry—in particular, on the hydrophilicity of the sample.[18–23] FN in solution is in a compact conformation.[16,37] The copolymer substrates employed in this work are based on the random

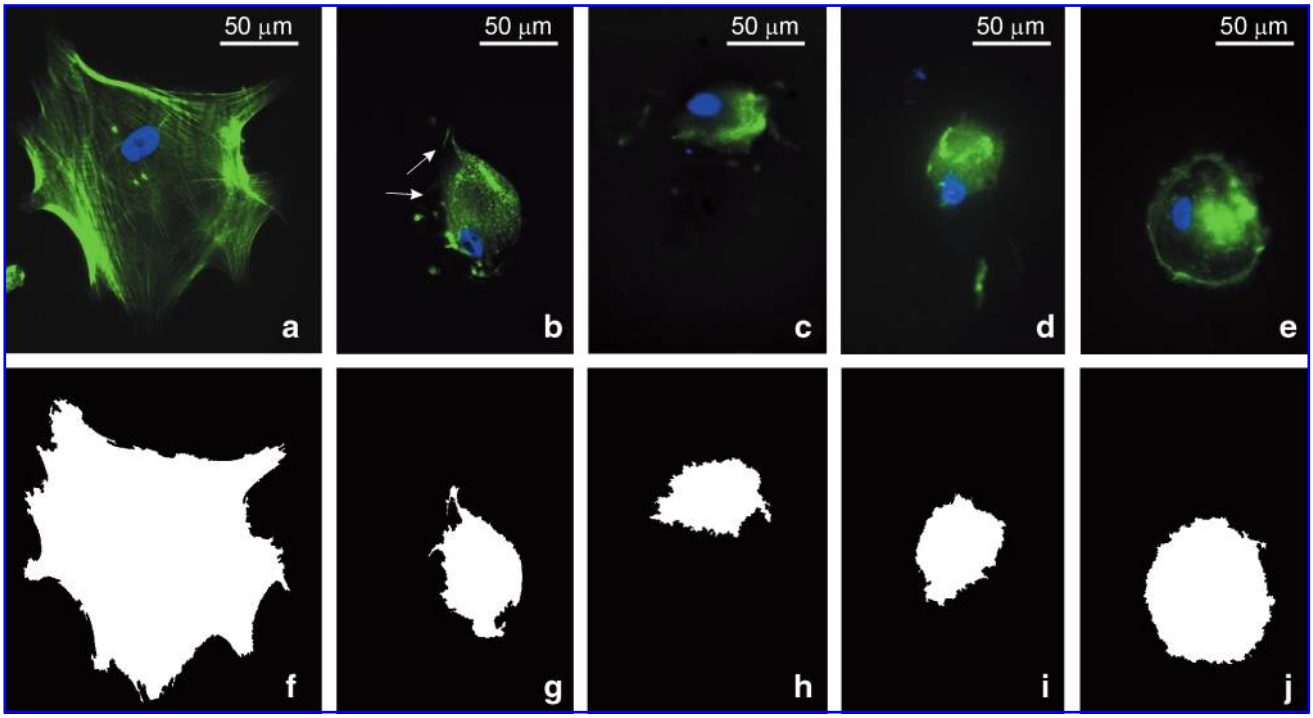


**FIG. 5.** F-actin cytoskeleton after 6 h of culture on substrates with increasing fraction of hydroxyl groups. (**a**) Poly(ethyl acrylate) (PEA), $x_{OH}=0$, (**b**) $x_{OH}=30$, (**c**) $x_{OH}=50$, (**d**) $x_{OH}=70$, and (**e**) poly(hydroxyethyl acrylate) (PHEA), $x_{OH}=1$. The arrow shows the incipient formation of actin fibers. Nuclei were counterstained with 4′,6-diamidino-2-phenylindole. (**f–j**) Images analysis of the previous cells from which the circularity parameter is calculated to quantify cell shape (Table 4). Color images available online at www.liebertonline.com/ten.

Table 4. Circularity as Calculated on Cells Cultured on Surfaces with Different OH Fraction from Image Analysis Shown in Figure 5

| $x_{OH}$ | *Circularity* |
|---|---|
| 0.0 | 0.19 |
| 0.3 | 0.20 |
| 0.5 | 0.21 |
| 0.7 | 0.32 |
| 1.0 | 0.35 |

combination of ethyl acrylate and hydroxyethyl acrylate monomers, which have a vinyl backbone chain with the side groups $-COOCH_2CH_3$ and $-COOCH_2CH_2OH$, respectively. Their copolymerization gives rise to a substrate in which the surface density of −OH groups can be varied without modifying any other chemical functionality of the system. The concentration of −OH groups determines both the surface energy and the hydrophilicity of the substrate (Table 1). The interaction of the protein domains with the chemical functionalities of the substrate and with water determines the molecule's adsorbed conformation. Topography of the surfaces examined by AFM prior protein adsorption yielded similar roughness parameters regardless the polymer composition. Besides, we also scanned the surface of the materials after immersion in the physiological solution (i.e., without FN) with no difference when they were compared to the surfaces before adsorption. Also, the stiffness of the different substrates, which is known to have a profound effect on cell adhesion, does not vary significantly among our substrates as measured by nanoindentation making use of AFM.[38,39]

FN is able to form a network on the more hydrophobic surfaces (i.e., PEA, $-OH_{90}$, $-OH_{80}$, and $-OH_{70}$) whose density decreases as the fraction of the hydroxyl groups on the surface increases. Protein interconnection degree has been quantified by the fractal dimension of the AFM images (Table 3). Fractal dimension is a parameter frequently used to analyze textures at different scales. The value of the two-dimensional fractal dimension is closely related to structural properties like porosity, complexity, and connectivity.[31] Fibrillogenesis, the formation of an FN network, has been described as a process driven by cells that occurs when integrins interact with the adequate domains of the FN protein and extend their subunits giving rise to the formation of a network of fibrils.[27] It has been shown that existence of mechanical tension is necessary for efficient integrin-mediated FN fibrillogenesis.[40,41] Fibrillar networks of FN have been generated also in the absence of cells, by means of interactions with the underlying substrate that involves mechanical events at the molecular scale. FN fibrillogenesis upon contact with a lipid monolayer was explained through mechanical tension caused by domain separation in the lipid monolayer that pulls the protein into an extended conformation.[42] Recently, the assembly of FN into fibers was obtained by applying forces to FN molecules via poly dimethylsiloxane (PDMS) micropillars at different stages of fibrillogenesis.[43] Our results show that FN fibrillogenesis can take place as a consequence of the sole interaction between the protein molecules and a material surface with the appropriate surface chemistry. Moreover, this material-induced fibrillogenesis depends strongly on the amount of protein adsorbed on the substrate: as the protein is adsorbed on the material substrate from more concentrated solutions, its distribution on the substrate changes from a globular-like morphology to a more elongated one and, finally, the formation of the protein network takes place. Table 2 shows the increase in the fractal dimension of the sketelonised AFM images (Fig. 3) as the concentration of the solution increases. From a certain concentration of hydroxyl groups in the substate on ($x_{OH} = 0.5$), the interaction between FN domains and the substrate surface keeps the protein molecules in a globular-like conformation, and the protein network is not formed anymore. It must be taken into account that our AFM measurements were performed after drying the surface of the samples after FN adsorption, which might also play a role in the fibrillogenesis process. Nevertheless, we have recently started measurements in wet conditions, and some evidence for fibrillar aggregation has already been found.

FN conformation on the substrate is not related to the total amount of protein adsorbed on it. Protein quantification from image analysis of Western blot bands shows a non-monotonic dependence of the FN surface density on the fraction of hydroxyl groups in the sample. It is shown that independently of the solution concentration from which the protein is adsorbed, FN adsorbs preferentially on the more hydrophilic and hydrophobic substrates. Then, at the intermediate −OH fractions, the amount of protein adsorbed decreases and reaches a minimum at approximately $x_{OH} = 0.5$. This nonmonotonic dependence of adsorbed protein on −OH fraction can be understood if protein adsorption on a substrate's surface is analyzed in terms of the number of available sites on the surface; it is clear that not only the energetic interactions between the substrate and the protein play a role in the adsorption process, but also the conformation of the protein—the configurational entropy—must trigger the amount of molecules directly adsorbed on the substrate: globular conformations of FN on the more hydrophilic substrates must lead to a higher amount of the protein adsorbed. The other way around, minimum adsorption at

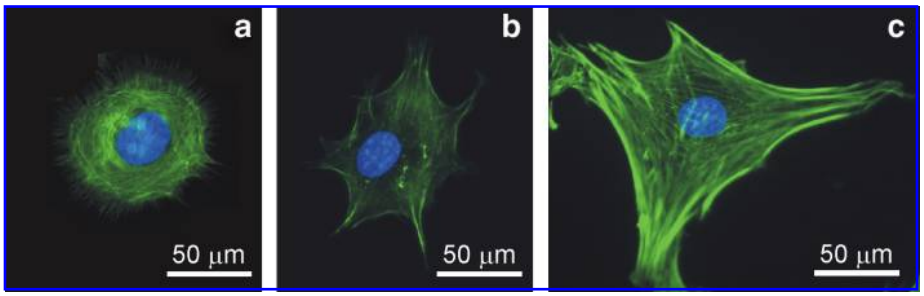


**FIG. 6.** F-actin cytoskeleton after different culture times on the most hydrophobic substrate ($x_{OH} = 0$). (**a**) 30 min, (**b**) 90 min, and (**c**) 180 min. Nuclei were counterstained with 4′, 6-diamidino-2-phenylindole. Color images available online at www.liebertonline.com/ten.

$x_{OH} = 0.5$ must be a consequence of two opposite processes: energetic and entropic interactions that lead to less efficient FN packing for this substrate composition.

The different conformations of FN on the surfaces must influence the biological performance of the substrates: the interaction between FN domains and the cell is regulated by several cell membrane receptors (mainly integrins and other non-integrin binding proteins).[40–44] Protein density on the substrate, as well as its conformation, modifies the availability of the binding sequences of FN to cell receptors and influences the biological success of the artificial substrate. First, some integrin receptors recognize specific peptide sequences in the protein, and their binding is strongly affected by the quantity, distribution, and spatial orientation of those sequences. Disruption of the secondary structure might alter the local topology of integrin-binding sequences or alter distances between cooperative sites, reducing integrin binding affinity.[41–45] Our results stress the difference between the total amount of FN adsorbed on a substrate and its conformation, especially concerning initial cell adhesion. Figure 5 shows the actin cytoskeleton development—and indirectly cell morphology—in primary human osteoblasts after 6 h of culture in serum-free medium on the previously FN-coated substrates. Cells are more spread—and with more developed actin fibers—on the most hydrophobic substrate (Fig. 5a), that is, the one that enhances most FN–FN interactions leading to the substrate-induced fibrillogenesis phenomenon. Cell morphology was quantified by means of image analysis (Fig. 5). Circularity increases as the hydrophilicity of the sample increases, suggesting more rounded-like shapes of cells (Table 4). That is to say, cells are able to spread on the most hydrophobic substrate after 3 h, as the dynamics of cell adhesion shown in Figure 6 suggest, which does not take place on the rest of substrates even after 6 h of culture. Moreover, cell spreading as well as the polymerization of the actin cytoskeleton are well correlated with cell adhesion. The formation of actin seems to be a necessity for the development of integrin adhesions.[42,46] Integrin receptors physically interact with the actin cytoskeleton[43,44,47,48] and stress fibers of actin function as transmitters of forces.[45,49] It has been shown that focal contact formation was inhibited when actin filaments were disrupted.[46,50,51]

Even though similar amounts of protein are adsorbed on the most hydrophilic substrate, as shown on the graph in Figure 2, the very different FN conformation in both situations (compare Fig. 4a and 4g) leads to a poorer cell adhesion as it is shown by the slower dynamics in the actin cytoskeleton formation: cell in Figure 5e is in the initial stages of actin cytoskeleton development, as shown by the green surrounding border along the cell periphery.[42,46] For intermediate fractions of hydroxyl groups on the surface, the actin development is in between the more hydrophilic and hydrophobic situations. Clearly, cell adhesion is better for the $-OH_{70}$ substrate. Figure 5b shows more advanced actin polymerization, where some incipient fibers are marked with arrows. It is remarkable that this surface composition ($x_{OH} = 0.3$) is the last one where the FN network is formed (see Fig. 4). Finally, for the $-OH_{50}$ and $-OH_{30}$ substrates, on which the protein is adsorbed in globular-like aggregates, the polymerization of actin fibers is delayed compared with the substrates that induce FN fibrillogenesis. Once again, the total amount of FN adsorbed on the surface is not the clue factor that influences osteoblast adhesion: while the same protein surface density is found on the $-OH_{30}$ and $-OH_{70}$ (Fig. 2) samples, the first one is able to induce the formation of a protein network, but the second one does not (Fig. 4d, f), and the degree of actin cytoskeleton formation and, as a consequence, cell adhesion are better on the first substrate.

## Conclusions

The influence of surface hydroxyl group density on FN protein adsorption has been investigated. FN is capable of establishing FN–FN interactions that lead to the formation of a protein network, that is, a substrate-induced fibrillogenesis process. This phenomenon is strongly dependent upon the surface chemistry and only takes place for those substrates with hydroxyl fraction lower than $x_{OH} = 0.7$. Moreover, we have compared protein conformation and protein density—as obtained from quantification of Western blot bands of the protein after adsorption on the different substrates—with osteoblast adhesion. The total amount of FN on the substrates reaches a minimum for intermediate hydroxyl fractions in the sample. That is to say, though nearly the same amount of FN is adsorbed on the substrates with the lowest and the highest hydroxyl density, only those substrates with $x_{OH} < 0.7$ are able to induce fibrillogenesis and it is precisely on these substrates where cell adhesion is better.

Our results could have direct implications in the use of biomaterials in tissue engineering strategies. In a practical point of view, this work might be useful in improving methodologies of precoating substrates (including scaffolds) with adhesive proteins; for uncoated substrates it might provide indications for future works related to the investigation of the influence of surface chemistry and wettability on the spatial organization of proteins that are adsorbed onto the biomaterials' surfaces immediately before cell attachment.

## Acknowledgments

AFM was performed under the technical guidance of the Microscopy Service at the Universidad Politécnica de Valencia, whose advice is greatly appreciated.

The support of the Universidad Politécnica de Valencia through Project No. 5696 and the Spanish Ministry of Science through Project No. MAT2006-08120 (including the Fondo Europeo de Desarrollo Regional [FEDER] financial support) are kindly acknowledged. "This work was partly financed through convenio de colaboración entre el Instituto de Salud Carlos III, la Conselleria de Sanidad de la Generalitat Valenciana y la Fundación de la Comunidad Valenciana Centro de Investigación Principe Felipe para la investigación bãsica y traslacional en medicina regenerativa."

## Disclosure Statement

No competing financial interests exist.

## References

1. Gumbiner, B.M. Cell adhesion: the molecular basis of tissue architecture and morphogenesis. Cell **84,** 345, 1996.
2. Anselme, K. Osteoblast adhesion on biomaterials. Biomaterials **21,** 667, 2000.

3. García, A.J. Interfaces to control cell-biomaterial adhesive interactions. Adv Polym Sci **203,** 171, 2006.
4. Werner, C., Pompe, T., and Salchert, K. Modulating extracellular matrix at interfaces of polymeric materials. Adv Polym Sci **203,** 63, 2006.
5. Keselowsky, B.G., Collard, D.M., and García, A.J. Surface chemistry modulates fibronectin conformation and directs integrin binding and specificity to control cell adhesion. J Biomed Mater Res A **66,** 247, 2003.
6. Michael, K.E., Vernekar, V.N., Keselowsky, B.G., Meredith, J.C., Latoru, R.A., and García, A.J. Adsorption-induced conformational changes in fibronectin due to interactions with well-defined surface chemistries. Langmuir **19,** 8033, 2003.
7. Tsapikouni, T.S., and Missirlis, Y.F. pH and ionic strength effect on single fibrinogen molecule adsorption on mica studied with AFM. Colloid Surface B **57,** 89, 2007.
8. Benesch, J., Hungerford, G., Suhling, K., Tregidgo, C., Mano, J.F., and Reis, R.L. Fluorescence probe techniques to monitor protein adsorption-induced conformation changes on biodegradable polymers. J Colloid Interface Sci **312,** 193, 2007.
9. Weber, N., Pesnell, A., Bolikal, D., Zeltinger, J., and Kohn, J. Viscoelastic properties of fibrinogen adsorbed to the surface of biomaterials used in blood-contacting medical devices. Langmuir **23,** 3298, 2007.
10. Steiner, G., Tunc, S., Maitz, M., and Salzer, R. Conformational changes during protein adsorption. FT-IR spectroscopic imaging of adsorbed fibrinogen layers. Anal Chem **79,** 1311, 2007.
11. Lord, M.S., Stenzel, M.H., Simmons, A., and Milthorpe, B.K. The effect of charged groups on protein interactions with poly(HEMA) hydrogels. Biomaterials **27,** 567, 2006.
12. Noh, H., and Vogler, E.A. Volumetric interpretation of protein adsorption: mass and energy balance for albumin adsorption to particulate adsorbents with incrementally increasing hydrophilicity. Biomaterials **27,** 5801, 2006.
13. Prime, L., and Whitesides, G.M. Self-assembled organic monolayers: model systems for studying adsorption of proteins at surfaces. Science **252,** 1164, 1991.
14. Sousa, S.R., Manuela Brás, M., Moradas-Ferreira, O., and Barbosa, M.A. Dynamics of fibronectin adsorption on $TiO_2$ surfaces. Langmuir **23,** 7046, 2007.
15. Erickson, H.P., and McDonagh, J. Fibronectin molecule visualized in electron microscopy: a long, thin, flexible strand. J Cell Biol **91,** 673, 1981.
16. Erickson, H.P., and Carell, N.A. Fibronectin in extended and compact conformations. Electron microscopy and sedimentation analysis. J Biol Chem **258,** 14539, 1983.
17. Pearlstein, E., Gold, L.I., and Garcia-Pardo, A. Fibronectin: a review of its structure and biological activity. Mol Cell Biochem **23,** 103, 1980.
18. García, A.J., and Boettiger, D.B. Integrin–fibronectin interactions at the cell-material interface: initial integrin binding and signaling. Biomaterials **20,** 2427, 1999.
19. Toworfe, G.K., Composto, R.J., Adams, C.S., Shapiro, I.M., and Ducheyne, P. Fibronectin adsorption on surface-activated poly(dimethylsiloxane) and its effect on cellular function. J Biomed Mater Res A **71,** 449, 2004.
20. Baugh, L., and Vogel, L. Structural changes of fibronectin adsorbed to model surfaces probed by fluorescence resonance energy transfer. J Biomed Mater Res A **69,** 525, 2004.
21. Lan, M.A., Gersbach, C.A., Michael, K.E., Keselowsky, B.G., and García, A.J. Myoblast proliferation and differentiation on fibronectin-coated self assembled monolayers presenting different surface chemistries. Biomaterials **26,** 4523, 2005.
22. Grinnell, F., and Feld, M.K. Fibronectin adsorption on hydrophilic and hydrophobic surfaces detected by antibody binding and analyzed during cell adhesion in serum-containing medium. J Biol Chem **257,** 4888, 1982.
23. Altankov, G., Thom, V., Groth, T., Jankova, K., Jonsson, G., and Ulbricht M. Modulating the biocompatibility of polymer surfaces with poly(ethylene glycol): effect of fibronectin. J Biomed Mater Res A **52,** 219, 2000.
24. Kowalczynska, H.M., Nowak-Wyrzykowska, M., Kolos, R., Dobkowski, J., and Kaminski, J. Fibronectin adsorption and arrangement on copolymer surfaces and their significance in cell adhesion. J Biomed Mater Res A **72,** 228, 2005.
25. Khang, D., Yeol, K., Liu-Snyder, P., Palmore, T.R., Durbin, S.M., and Webster, T.J. Enhanced fibronectin adsorption on carbon nanotube/poly(carbonate) urethane: independent role of surface nano-roughness and associated surface energy. Biomaterials **28,** 4759, 2007.
26. Costa Martínez, E., Rodríguez Hernandez, J.C., Machado, M., Mano, J.F., Gómez Ribelles, J.L., Monleón Pradas, M., and Salmerón Sánchez, M. Human chondrocyte morphology, its dedifferentiation and fibronectin conformation on different PLLA microtopographies. Tissue Eng **14,** 1751, 2008.
27. Mao, Y., and Schwarzbauer, J.E. Fibronectin fibrillogenesis, a cell-mediated matrix assembly process. Matrix Biol **24,** 389, 2005.
28. Otsu, N. A threshold selection method from gray-level histograms. IEEE Trans Syst Man Cybern **9,** 62, 1979.
29. Soille, P., and Rivest, J.-F. On the validity of fractal dimension measurements in image analysis. J Vis Commun Image R **7,** 217, 1996.
30. Keller, J.M., Chen, S., and Crownover, R.M. Texture description and segmentation through fractal geometry. Comput Vis Graph Image Process **45,** 150, 1989.
31. Pothuaud, L., Benhamou, C.L., Porion, P., Lespessailles, E., Harba, R., and Levitz, P. Fractal dimension of trabecular bone projection texture is related to three-dimensional microarchitecture. J Bone Miner Res **15,** 691, 2000.
32. Gonzalez, R.C, Woods, R.E., and Eddins, S.L. Digital Image Processing Using MATLAB. Upper Saddle River, NJ: Prentice-Hall, 2003.
33. Gonzalez, R.C., and Woods, R.E. Digital Image Processing. Upper Saddle River, NJ: Prentice-Hall, 2007.
34. MATLAB Image Processing Toolbox User's Guide. Natick, MA: The MathWorks, Inc., 2006.
35. Alberts, B., Johnson, A., Lewis, J., Raff, M., Roberts, K., and Watson, J.D. Molecular Biology of the Cell. New York: Garland Science, 916–982, 2002.
36. Altankov, G., and Groth, T. Reorganization of substratum-bound fibronectin on hydrophilic and hydrophobic materials is related to biocompatibility. J Mater Sci Mater Med **5,** 732, 1994.
37. Altankov, G., and Groth, T. Fibronectin matrix formation and the biocompatibility of materials. J Mater Sci Mater Med **7,** 425, 1996.
38. Salmerón Sánchez, M., Molina Mateo, J., Romero Colomer, F.J., and Gómez Ribelles, J.L. Nanoindentation and tapping mode AFM study of phase separation in poly(ethyl acrylate-co-hydroxyethyl methacrylate) copolymer networks. Eur Polym J **42,** 1378, 2006.
39. Rodríguez Hernández, J.C., Salmerón Sánchez, M., Gómez Ribelles, J.L., and Monleón Pradas, M. Polymer-silica nanocomposites prepared by sol-gel technique: nanoindentation and tapping mode AFM studies. Eur Polym J **43,** 2275, 2007.

40. Erickson, H.P. Stretching fibronectin. J Muscle Res Cell Motil **23,** 575, 2002.
41. Smith, M.L., Gourdon, D., Little, W.C., Kubow, K.E., Eguiluz, R.A., Luna-Morris, S., and Vogel, V. Force-induced unfolding of fibronectin in the extracellular matrix of living cells. PLoS Biol **5,** e268, 2007.
42. Baneyx, G., and Vogel, V. Self-assembly of fibronectin into fibrillar networks underneath dipalmitoyl phosphatidylcholine monolayers: role of lipid matrix and tensile forces. Proc Natl Acad Sci USA **96,** 12518, 1999.
43. Ulmer, J., Geiger, B., and Spatz, J.P. Force-induced fibronectin fibrillogenesis *in vitro*. Soft Mater **4,** 1998, 2008.
44. Johnson, K.J., Sage, H., Briscoe, G., and Erickson, H.P. The compact conformation of fibronectin is determined by intramolecular ionic interactions. J Biol Chem **274,** 15473, 1999.
45. Potts, J.R., and Campbell, I.D. Structure and function of fibronectin modules. Matrix Biol **15,** 313, 1996.
46. Lewandowska, K., Pergament, E., Sukenik, C.N., and Culp, L.A. Cell-type-specific adhesion mechanisms mediated by fibronectin adsorbed to chemically derivatized substrata. J Biomed Mater Res **26,** 1343, 1992.
47. Lüthen, F., Lange, R., Becker, P., Rychly, J., Beck, U., and Nebe, J.G.B. The influence of surface roughness of titanium on β1- and β3-integrin adhesion and the organization of fibronectin in human osteoblastic cells. Biomaterials **26,** 2423, 2005.
48. Nebe, B., Bohn, W., Sanftleben, H., and Rychly, J. Induction of a physical linkage between integrins and the cytoskeleton depends on intracellular calcium in an epithelial cell line. Exp Cell Res **229,** 100, 1996.
49. Nebe, B., Bohn, W., Pommerenke, H., and Rychly, J. Flow cytometric detection of the association between cell surface receptors and the cytoskeleton. Cytometry **28,** 66, 1997.
50. Schmidt, C., Pommerenke, H., Duerr, F., Nebe, B., and Rychly, J. Mechanical stressing of integrin receptors induces enhanced tyrosine phosphorylation of cytoskeletally anchored proteins. J Biol Chem **273,** 5081, 1998.
51. Riveline, D., Zamir, E., Balaban, N.Q., Schwarz, U.S., Ishizaki, T., Narumiya, S., Kam, Z., Geiger, B., and Bershadsky, A.D. Focal contacts as mechanosensors externally applied local mechanical force induces growth of focal contacts by an mDia1-dependent and ROCK-independent mechanism. J Cell Biol **153,** 1175, 2001.

Address correspondence to:
*Manuel Salmerón-Sánchez, Ph.D.*
*Center for Biomaterials and Tissue Engineering*
*Universidad Politécnica de Valencia*
*Camino de Vera s/n*
*46022 Valencia*
*Spain*

*E-mail:* masalsan@fis.upv.es

*Received: March 2, 2009*
*Accepted: April 21, 2009*
*Online Publication Date: June 12, 2009*